



Contents lists available at ScienceDirect

Structures

journal homepage: www.elsevier.com/locate/structures

Load-Carrying Capacity of End Cross-Girder with Inspection Holes in Composite Bridge

Eiki Yamaguchi *, Hiroyuki Tsuji

Dept. of Civil Engineering, Kyushu Institute of Technology, Kitakyushu, Japan

ARTICLE INFO

Article history:

Received 15 May 2016

Received in revised form 18 November 2016

Accepted 19 December 2016

Available online xxx

Keywords:

End cross-girder

Corrosion

Inspection hole

Load-carrying capacity

Finite element analysis

ABSTRACT

A severely corroded end cross-girder is found occasionally, while the girder is expected to play an important role under seismic loading. The prevention of the end cross-girder against corrosion is therefore crucial in the bridge maintenance. To this end, the present research aims at improving its inspectability by installing inspection holes in the end cross-girder. The influences of the holes on the load-carrying capacity are then studied, to be specific. It is revealed that the inspection holes would reduce the load-carrying capacity considerably; the degree of the influence varies with the shape, the position and the size of the hole. Six reinforcement methods are therefore considered. Full recovery of the capacity turns out to be possible if the inspection hole is the same size as that of the standard opening (manhole) in a steel bridge structure, while it is not an easy task when the inspection hole is larger.

© 2016 Institution of Structural Engineers. Published by Elsevier Ltd. All rights reserved.

1. Introduction

Cross girders or cross frames at the girder end are essential structural elements for the bridge to resist earthquakes. The current Japanese specifications for highway bridges require that the end cross-girder be large and strong with its lower flange as close to the lower flange of the main girder as possible [1]. In Chile, bridges with no end cross-girders or no end cross-frames had been constructed, many of which were damaged badly by the earthquake in 2010 [2]. The incident has demonstrated the importance of the end cross-girder/end cross-frame for the earthquake resistance.

The severe corrosion of the steel bridge has occurred mostly at the girder end [3]. This is attributed to water leakage through the expansion joint and the formation of congested space at the girder end. In short, corrosion environment is quite bad around the end cross-girder.

The corrosion reduces the cross sectional area, which deteriorates the load-carrying capacity of the member [4–6]. Many steel bridges were replaced in Japan because safety was threatened by corrosion [7]. Thus the protection of a steel bridge from corrosion is a very important issue for bridge maintenance.

The corrosion of the end cross-girder can reduce the safety margin of a bridge and can endanger a bridge during large earthquake. Nevertheless, the girder end is often exposed to corrosive environment. More careful inspection is therefore required for the girder end than for the other members. Quite frequently, however, the distance between the end cross-girder and the parapet is so small that visual inspection on the parapet side is practically impossible. This creates a situation

where the corrosion is not noticed until it penetrates through the plate of the end cross-girder and holes are made. Photo 1 shows an example of such an end cross-girder. In this bridge, in addition to the partial loss of the cross section of the web, the severe reduction in the flange thickness on the parapet side had been caused, but it was recognized only after the repair work was started.

Against the background of the information above, the end cross-girder with inspection holes in the web is proposed. The holes enable one to conduct visual inspection of the parapet side of the girder. In addition, the improvement of ventilation can be expected as well.

However, the inspection holes would inevitably degrade the load-carrying capacity of the end cross-girder. In the present study, the reduction in the capacity is evaluated and the reinforcement method to make it up is then investigated.

2. End cross-girder model

Referring to the bridge in the textbook on composite-bridge design [8], the end cross-girder shown in Fig. 1 is employed for the present study. The whole end cross-girder and the parts of the main girders are taken out to construct the end cross-girder model. The end portion of each main girder, the length of which is 220 mm, is used in this end cross-girder model. It is noted that the textbook intends to provide a standard design procedure so that the present end cross-girder model is a typical one.

Young's modulus of steel E and Poisson's ratio ν are 2.0×10^5 N/mm² and 0.3, respectively. The yield stress σ_y of the main girder is 355 N/mm² and that of the end cross-girder 235 N/mm². The material behavior of the steel is elastic-plastic of von Mises type with the kinematic hardening rule. The uniaxial stress-strain relationship in

* Corresponding author.

E-mail address: yamaguch@civil.kyutech.ac.jp (E. Yamaguchi).



Fig. 1. End cross-girder.

tension is described by the bilinear curve with the second slope of $E/100$, which is the material modeling commonly employed for steel members [9].

The horizontal load is applied to the upper flange as uniformly distributed load as well as the dead load of concrete slab. The horizontal load is the inertia force of the concrete slab, by which the basic characteristics of the mechanical behavior of the end-cross girder during earthquake is studied. Since only the end cross-girder is analyzed instead of the whole bridge, some constraints are imposed on the movements of the upper flange of the end cross-girder so that the end cross-girder does not topple laterally: the rotation around the flange-axis (the axis normal to the bridge-axis) and the lateral displacement in the direction of the bridge-axis are not allowed, to be specific. It is noted that in the composite bridge the concrete slab prevents the end cross-girder from toppling laterally.

Fig. 1(a) is the view of the parapet side of the end cross-girder. The arrows in this figure indicate the loading direction. The lateral stiffener and the longitudinal stiffeners are placed on the other side of the girder. The stiffeners are therefore drawn by the dotted lines in this figure. Due to the transverse stiffener at the center of the web and the longitudinal stiffeners, the web can be considered to have two panels: the left panel is named Panel L and the right one Panel R as shown in Fig. 2. Note that all the figures in this paper are the views of the parapet side.

3. End cross-girder model with inspection holes

According to the survey by Nakai et al. [10], the standard size of the opening (manhole) in a steel bridge structure is 600 mm in height and 400 mm in width. 95% of the existing manholes are of this size. There are two types in terms of the shape: one has straight left and right sides with semicircular top and bottom sides; and the other is a rectangular hole with rounded corners. 62% of the existing manholes are of the former type and the remaining 38% are of the latter type. The radius of the

semicircular side in the former is 200 mm and that of the rounded corner in the latter is 100 mm.

Four end cross-girder models shown in Fig. 3 are constructed for the present study. The inspection holes in Models A and B are of the size identical to that of the standard manhole described above: the hole in Model A is of the semicircular type and the hole in Model B is of the rounded-corner type. Two inspection holes are made in each model, one in Panel L and the other in Panel R. The two inspection holes are located in the symmetric positions with respect to the web center. This is because the seismic loading is cyclic.

The size of the standard manhole is the minimum for a man to pass through without much trouble. For a better inspection in practice, larger holes are preferred. From this viewpoint, another two end cross-girder models, Models C and D are constructed in addition. The holes in these two models are of the same, size 800 mm in height and 530 mm in width. The hole shape in Model C is the same as that of Model A while that of Model D the same as that of Model B.

The position of the hole may influence the load-carrying capacity, which therefore needs to be investigated. “a” and “b” in Fig. 3 are utilized to specify the position of the inspection hole. Because of the stiffeners, the values of these parameters are bounded. The holes in Models C and D are so large that they cannot move vertically. That is why only “a” is given in Fig. 3(c) and (d).

In the present study, the following values are assigned to “a” and “b” for Models A and B: a = 25, 350, 675 mm, b = 25, 135, 245 mm. The combination of these values yields 9 different end cross-girders for each of Models A and B. For Models C and D, “a” takes 25, 302.5, 580 mm. Therefore there are three end cross-girder models for each of Models C and D. The name of the end cross-girder model uses the values of these parameters. For example, A-350-25 is Model A with a = 350 mm and b = 25 mm; and D-302.5 is Model D with a = 302.5 mm.

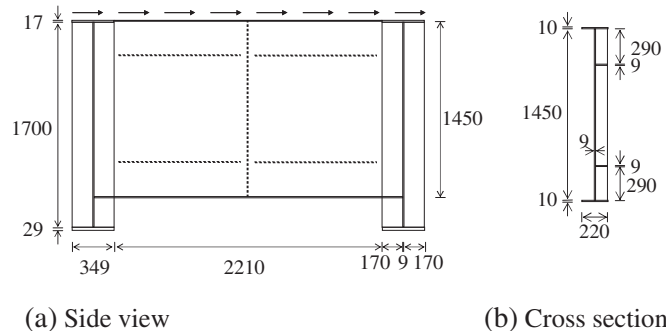


Fig. 2. Panels L and R in web.

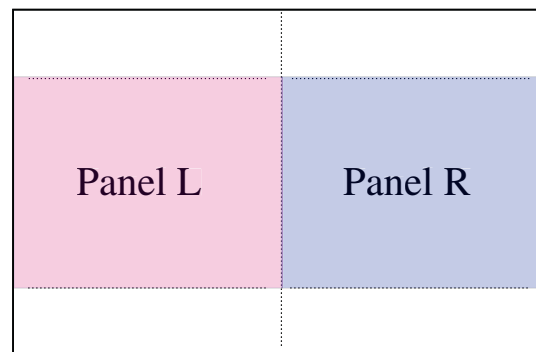
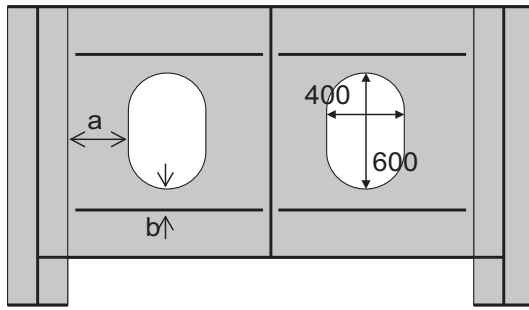
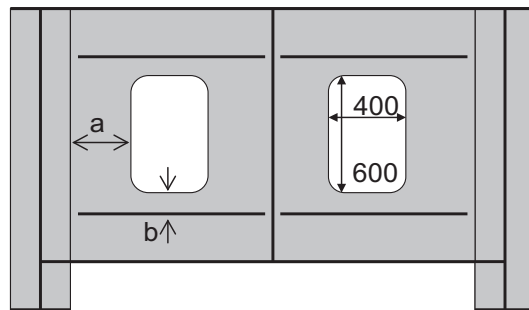


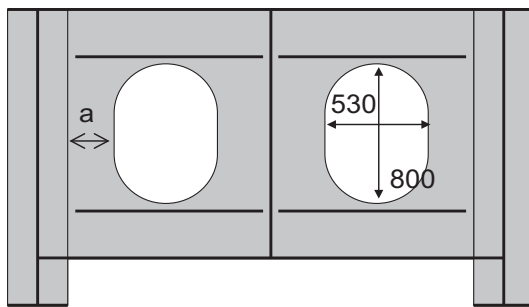
Fig. 3. End cross-girder model.



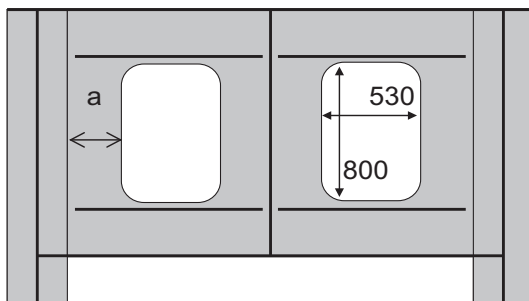
(a) Model A



(b) Model B



(c) Model C



(d) Model D

Fig. 4. Residual stress distribution.

4. Outline of analysis

The influence of inspection holes are investigated numerically. To that end, 3-D finite element analysis including the effects of material and geometrical nonlinearities is conducted. The initial imperfection, that is, residual stress and deformation, are also introduced in the analysis. The residual stress at the connection between the constituent plates is the yield stress σ_Y and the stress away from the connection $-0.3\sigma_Y$. The variation is assumed linear. The residual stress distribution herein is typical based on the book by Usami [11]. Needless to say, the residual stress state is in a state of self-equilibrium. The thermal stress analysis is carried out to implement the initial imperfection of the residual stress state first. Fig. 4 shows an example of the residual stress state thus implemented (the dotted line) with the targeted stress state (the solid line).

The mode of the lowest elastic buckling load is employed for the initial-deformation mode. It is obtained by the eigenvalue analysis. The magnitude of the deflection is the maximum permitted value for the fabrication error in the Japanese design codes for highway bridges [7]: the out-of-plane displacement of the web must be smaller than 1/250 of the web height.

ABAQUS [12] is used for all the analyses in the present study. The whole end-cross girder is modelled by the 4-node shell element "S4R". Most of the elements are square with a side length of 25 mm. The horizontal displacement at the center of the top flange is controlled to obtain the nonlinear load-displacement relationship.

5. Influence of inspection holes

The analysis results of load-carrying capacities P_{max} are given in Table 1, where P_0 is the capacity of the original end cross-girder (no inspection holes). The influence of the inspection holes are obvious: the presence of the holes reduces the load-carrying capacities considerably. P_{max}/P_0 of Model A becomes 58%–77% whereas that of Model B 54%–72%. The difference between the two models is attributable to the size

Table 1

Load-carrying capacity of end cross-girder with inspection holes.

Model	P_{max}/P_0
(a) Model A	
A-25-245	0.76
A-25-135	0.77
A-25-25	0.77
A-350-245	0.66
A-350-135	0.65
A-350-25	0.66
A-675-245	0.60
A-675-135	0.58
A-675-25	0.58
(b) Model B	
B-25-245	0.72
B-25-135	0.72
B-25-25	0.72
B-350-245	0.62
B-350-135	0.60
B-350-25	0.64
B-675-245	0.55
B-675-135	0.55
B-675-25	0.54
(c) Model C	
C-25	0.61
C-302.5	0.51
C-580	0.45
(d) Model D	
D-25	0.56
D-302.5	0.46
D-580	0.44

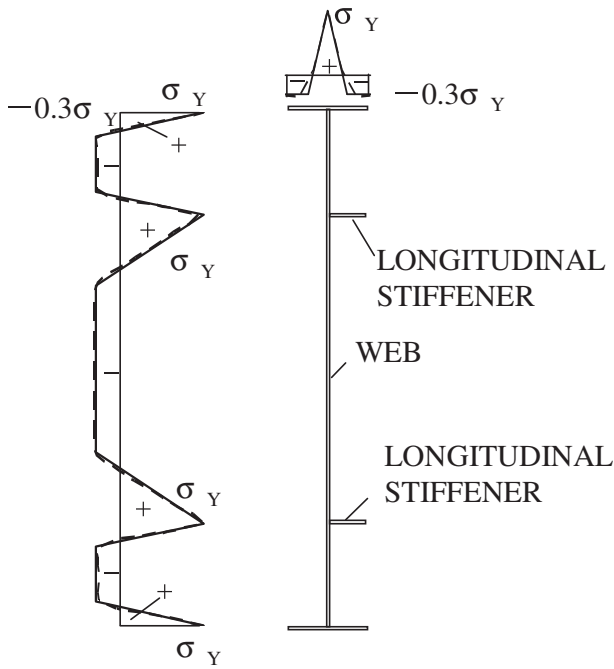
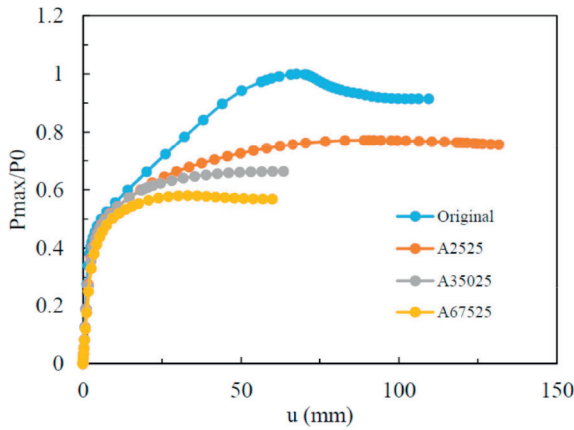
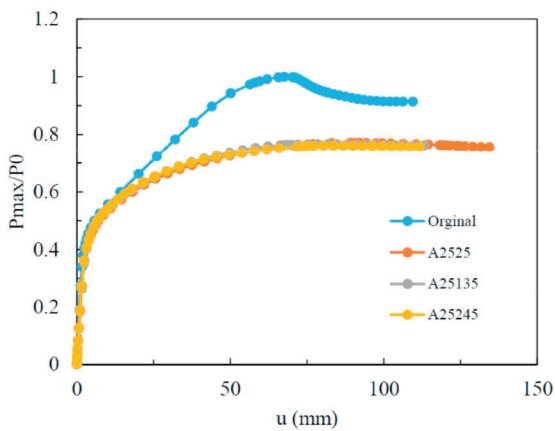


Fig. 5. Horizontal load-displacement relationship.



(a) Influence of horizontal position

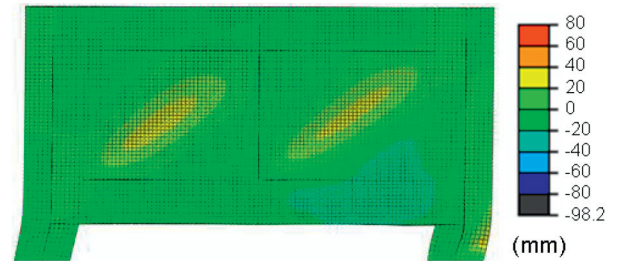


(b) Influence of vertical position

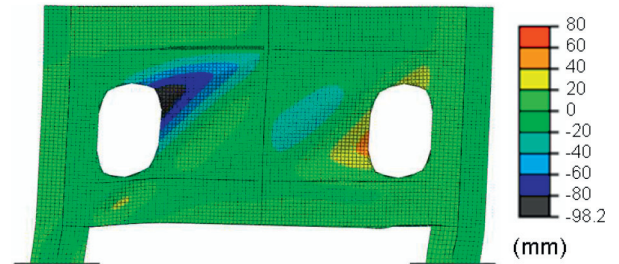
Fig. 6. Out-of-plane displacement.

of the hole area: The inspection hole in Model B is a little larger than that in Model A. The holes in Models C and D are much larger so that P_{max}/P_0 reduces to 45%–61% and 44%–56%, respectively.

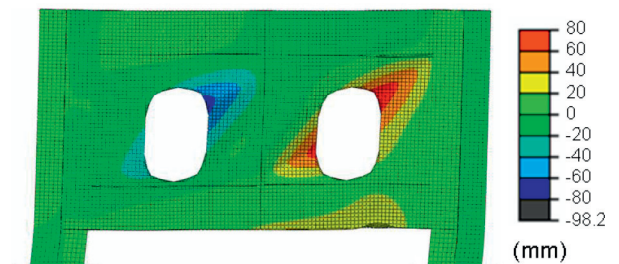
The influence of the inspection hole position on the load-carrying capacity can be clearly observed in Table 1 and also in Fig. 5 where u is the horizontal displacement at the center of the top flange: as the holes are getting closer to the web center, the reduction becomes larger, while the influence of the vertical position is found insignificant.



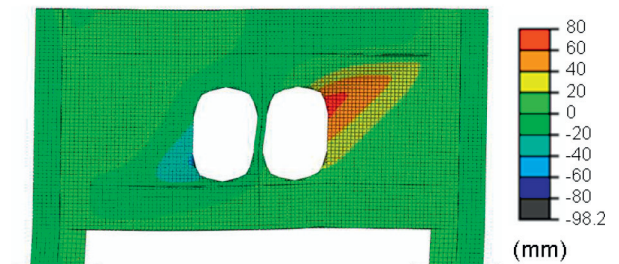
(a) Original



(b) A-25-25



(c) A-350-25



(d) A-675-25

Fig. 7. Reinforcement.

The out-of-plane displacement contours of the original end cross-girder, A-25-25, A-350-25 and A-675-25 are presented in Fig. 6. In the original end cross-girder, a diagonal tension field develops in each panel of the web. The diagonal tension fields are narrow and the out-of-plane displacement is not so large. With the inspection holes, the diagonal tension field is formed but in a very different fashion. It is clearly recognized that the position of the hole has a great influence on the formation of the diagonal tension field. In A-25-25, the holes are close to main girders, which work as if the reinforcement: the diagonal tension field develops only on one side of each hole. The shape of the field becomes very different and the out-of-plane displacement is larger, especially in Panel L, which is attributable to the smaller stiffness of the web plate due to the presence of the holes. A-350-25 causes two diagonal tension fields like in the original end cross-girder. But compared with the original end cross-girder, the deformed regions are wider and the out-of-plane displacement is larger as well. The two holes in A-675-25 appear to influence the deformation as if one big hole. The deformation of the transverse stiffener at the center of the web is observed. The out-of-plane displacement occurs in wide region and the magnitude is large.

The deformation characteristics of the other end-cross girder models are the same as those described above. These differences in the deformed configuration can explain the variation in the influence of the inspection hole on the load-carrying capacity.

The influence of the inspection hole is minimum when it is close to the main girder. Having the hole close to the main girder enables one to inspect the parapet side of the bearing as well. Therefore, it would be a good choice to set up the inspection hole close to the main girder; A-25-25, B-25-25, C-25 and D-25 are then considered in what follows.

6. Reinforcement

Widely-used reinforcement for the manhole under compression is the so-called doubling: the extra steel plate is attached around the manhole. 99% of the existing manholes have employed this reinforcement [10]. The remaining reinforcement is the combination of the stiffeners and the doubling [10]. The present study considers the doubling, the stiffeners and their combination. The effectiveness of these reinforcements has not been studied under the present loading condition of the horizontal force.

Following the current practice of manholes [10], the steel plate shown in Fig. 7(a) is installed around the manhole. This is for Model A. For the other models, the hole in the plate is adjusted to the relevant size and shape. A larger plate of 1600 mm in height and 1060 mm in width is employed for Models C and D. For the reinforcement by the stiffeners, the transverse stiffeners are attached along the sides of the hole, as the red lines in Fig. 7(b) indicate. The width of the stiffener is 100 mm.

The thickness of the doubling plate is 9 mm and that of the stiffener is 18 mm, both of which are standard for the reinforcement of the manhole. The 18-mm thick doubling plate and the 27-mm thick stiffener are

Table 2
Reinforcement.

Model	Plate thickness	
	Doubling	Stiffener
ReA	9	–
ReB	18	–
ReC	–	18
ReD	–	27
ReE	9	18
ReF	18	27

ReA, ReB: doubling.
ReC, ReD: stiffener.
ReE, ReF: combination.
Dimension: mm.

Table 3
Load-carrying capacity of reinforced end cross-girder with inspection holes.

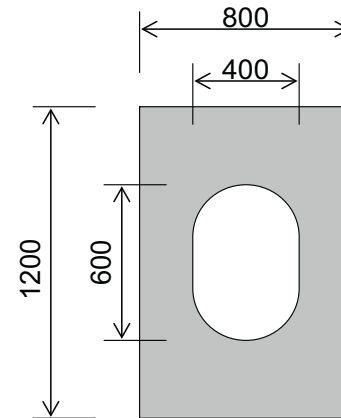
Reinforcement	P_{max}/P_0			
	A-25-25	B-25-25	C-25	D-25
ReA	0.98	0.90	0.89	0.78
ReB	0.98	–	–	–
ReC	0.87	0.79	0.69	0.60
ReD	0.87	–	–	–
ReE	0.99	1.00	0.90	0.88
ReF	0.99	–	–	–

also tested herein. Table 2 is the list of six reinforcements considered in the present study.

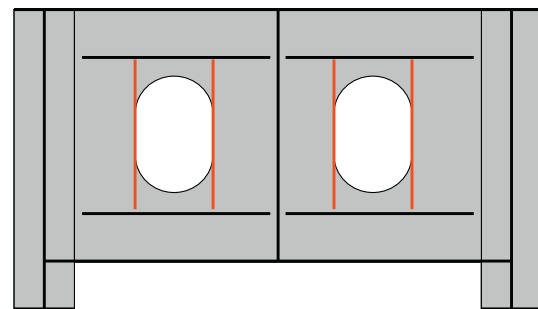
The effectiveness of these reinforcements is investigated numerically. Table 3 presents the load-carrying capacities of the reinforced end cross-girder models with the inspection holes. The results of A-25-25 reveal that the doubling is more effective than the stiffener; the standard thickness is strong enough; and the combination of the two helps recover almost full load-carrying capacity.

The out-of-plane displacement of the reinforced A-25-25 at P_{max} is shown in Fig. 8. The diagonal tension field is formed and yet the deformation characteristics such as the deformed region and the magnitude of the displacement are very different from those of the unreinforced girders shown in Fig. 6. The reinforcement thus changes the mechanical behavior considerably.

Following the results of A-25-25 regarding the plate thickness effect observed in Table 3, only the reinforcements of ReA, ReC and ReE are considered for the other end cross-girder models.

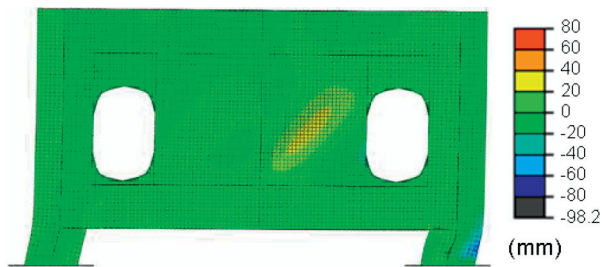


(a) Doubling plate (Model A)

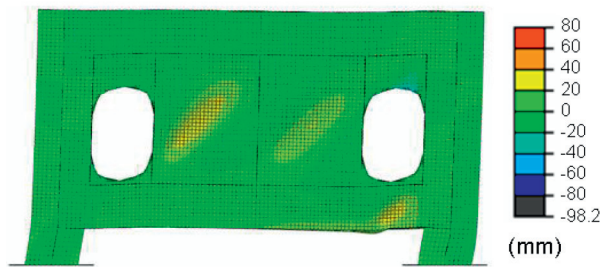


(b) Transverse stiffeners

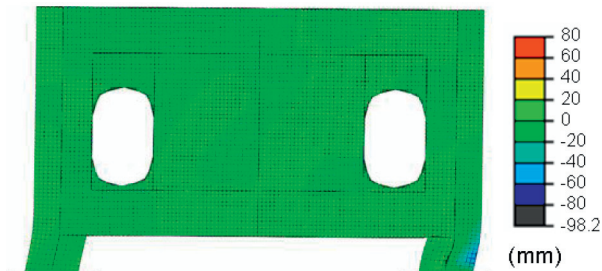
Fig. 8. Out-of-plane displacement of reinforced A-25-25.



(a) ReA



(b) ReC



(c) ReE

Photo 1. Severely corroded end cross-girder.

For B-25-25, the doubling is also found more effective, but the effectiveness is a little smaller. Yet the combination can recover the load-carrying capacity fully. C-25 and D-25, which undergo a large reduction in the load-carrying capacity, can recover only up to about $P_{\max}/P_0 = 90\%$ even by the combined reinforcement. The seismic design must be carried out more carefully when a large inspection hole is employed.

7. Concluding remarks

The end cross-girder plays a significant role against seismic loading, while it is located where corrosion tends to occur easily and the inspection is not necessarily easy to conduct. Against this background, the end

cross-girder with inspection holes were studied. In short, the load-carrying capacity of the end cross-girder under horizontal load was investigated by the 3-D nonlinear finite element analysis.

The following observations were made from the present study:

- (1) The inspection hole reduces the load-carrying capacity significantly: the larger the hole is, the greater the reduction becomes.
- (2) The influence of the inspection hole on the load-carrying capacity depends greatly on the horizontal position: as the hole approaches the center of the web, the reduction in the load-carrying capacity becomes larger.
- (3) Even though the loading condition is different, the standard reinforcements for a manhole help recover the load-carrying capacity of the end cross-girder with inspection holes.
- (4) For the reinforcement, the doubling is more effective than the stiffeners.
- (5) The standard plate thickness of the reinforcement for a manhole is sufficient. Further increase in the plate thickness does not improve the capacity.
- (6) When the size of the inspection hole is the same as that of the standard manhole, the doubling can recover the load-carrying capacity up to 90% of the original capacity. The combination of the doubling and the stiffener can achieve the almost full recovery.
- (7) For a larger inspection hole, even the combined reinforcement cannot recover the load-carrying capacity fully. Safety against seismic loading must be verified carefully.

Acknowledgements

The financial support for the present study, Grant-in-Aid for Scientific Research (C) (KAKENHI, No. 23560570), is gratefully acknowledged.

References

- [1] Japan Road Association. Specifications for highway bridges part 5 seismic design; 2012.
- [2] Chen G, et al. 2010 Chile Earthquake implications to the seismic design of bridges. Proceedings of the 26th US-Japan Bridge Engineering Workshop; 2010. p. 203–16.
- [3] Tamakoshi T, Nakasu K, Ishio K, Takeda T, Suizu N. Research on local corrosion of highway steel ridges. Technical Note of National Institute for Land and Infrastructure Management, No. 294; 2006.
- [4] Liu C, Miyashita T, Nagai M. Analytical study on shear capacity of steel I-girder with local corrosion nearby girder ends. J Struct Eng 2011;57A:715–23.
- [5] Khurrama N, Sasaki E, et al. Analytical demonstrations to assess residual bearing capacities of steel plate girder ends with stiffeners damaged by corrosion. Struct Infrastruct Eng 2012;1–11.
- [6] Yamaguchi E, Tsuji H. Influence of corrosion on performance of end cross girder under horizontal force. J Struct Eng 2014;60A:105–13.
- [7] Japan Road Association. Specifications for highway bridges part 2 steel bridges; 2012.
- [8] Japan Bridge Association. Design example and commentary of composite bridge; 2005.
- [9] Subcommittee on Steel Structures. Standard specifications for steel and composite structures, III design. Japan Society of Civil Engineers; 2007.
- [10] Nakai H, Horie Y, Kitada T, Iwai K, Suzuki I. Investigation of stiffened plates with opening under compression. Bridg Found 1996;30(9):31–8.
- [11] Usami T, editor. Guidelines for stability design of steel structures. 2nd ed. Japan Society of Civil Engineers; 2005.
- [12] ABAQUS. User's Manual, ABAQUS Ver. 6.8, Dassault Systemes Simulia Corp; 2008.